Large-scale differences in diversity and functional adaptations of prokaryotic communities from conserved and anthropogenically impacted mangrove sediments in a tropical estuary

Carolina O De Santana [Corresp., 1] , **Pieter Spealman** [2] , **Vania Melo** [3] , **David Gresham** [2] , **Taise de Jesus** [4] , **Eddy Oliveira** [4] , **Fabio Alexandre Chinalia** [1]

[1] Geosciences Institute, Federal University of Bahia, Salvador, Bahia, Brazil

[2] Department of Biology, New York University, New York City, New York, United States

[3] Department of Biology, Federal University of Ceará, Fortaleza, Ceará, Brazil

[4] Department of Biology, State University of Feira de Santana, Feira de Santana, Bahia, Brazil

Corresponding Author: Carolina O De Santana
Email address: cal.uefsbio@yahoo.com.br

Mangroves are tropical ecosystems with strategic importance for climate change mitigation on local and global scales. They are also under considerable threat due to fragmentation, degradation, and urbanization. However, a complete understanding of how anthropogenic actions can affect microbial biodiversity and functional adaptations is still lacking. In this study, we carried out 16S rRNA gene sequencing analysis using sediment samples from two distinct mangrove areas located within the Serinhaém Estuary, Brazil. The first sampling area was located around the urban area of Ituberá, impacted by domestic sewage and urban runoff, while the second was an environmentally conserved site. Our results show significant changes in the structure of the communities between impacted and conserved sites. Biodiversity, along with functional potentials for the cycling of carbon, nitrogen, phosphorus and sulfur, were significantly increased in the urban area. We found the environmental factors of organic matter, temperature and copper were significantly correlated with the observed shifts in the communities. Contributions of specific taxa to the functional potentials were negatively correlated with biodiversity, such that fewer numbers of taxa in the conserved area contributed to the majority of the metabolic potential. The results suggest that the contamination by urban runoff may have generated a different environment that led to the extinction of some taxa observed at the conserved site. In their place we find the impacted site is enriched in prokaryotic families that are known human and animal pathogens, a clear negative effect of the urbanization process.

1 **Large-scale differences in diversity and functional**
2 **adaptations of prokaryotic communities from conserved and**
3 **anthropogenically impacted mangrove sediments in a**
4 **tropical estuary**

6 Carolina Oliveira de Santana[1]; Pieter Spealman[2]; Vânia Maria Maciel Melo[3]; David Gresham[2];
7 Taise Bomfim de Jesus[4], Eddy José Francisco Oliveira[4], Fabio Alexandre Chinalia[1]

9 [1] Geosciences Institute, Federal University of Bahia, Salvador, Bahia, Brazil
10 [2] Department of Biology, New York University, New York City, New York, United States
11 [3] Department of Biology, Federal University of Ceará, Fortaleza, Ceará, Brazil
12 [4] Department of Biology, State University of Feira de Santana, Feira de Santana, Bahia, Brazil

14 Corresponding Author:

16 Carolina Oliveira de Santana[1]
17 Av. João Durval Carneiro - 150, Feira de Santana, Bahia, 44088-714, Brazil
18 Email address: cal.uefsbio@yahoo.com.br

Abstract

20 **Abstract**
21   Mangroves are tropical ecosystems with strategic importance for climate change mitigation on
22 local and global scales. They are also under considerable threat due to fragmentation, degradation, and
23 urbanization. However, a complete understanding of how anthropogenic actions can affect microbial
24 biodiversity and functional adaptations is still lacking. In this study, we carried out 16S rRNA gene
25 sequencing analysis using sediment samples from two distinct mangrove areas located within the
26 Serinhaém Estuary, Brazil. The first sampling area was located around the urban area of Ituberá, impacted
27 by domestic sewage and urban runoff, while the second was an environmentally conserved site. Our
28 results show significant changes in the structure of the communities between impacted and conserved
29 sites. Biodiversity, along with functional potentials for the cycling of carbon, nitrogen, phosphorus and
30 sulfur, were significantly increased in the urban area. We found the environmental factors of organic
31 matter, temperature and copper were significantly correlated with the observed shifts in the communities.
32 Contributions of specific taxa to the functional potentials were negatively correlated with biodiversity,
33 such that fewer numbers of taxa in the conserved area contributed to the majority of the metabolic
34 potential. The results suggest that the contamination by urban runoff may have generated a different
35 environment that led to the extinction of some taxa observed at the conserved site. In their place we find
36 the impacted site is enriched in prokaryotic families that are known human and animal pathogens, a clear
37 negative effect of the urbanization process.

38

39   **Introduction**

40   Mangrove forests are coastal ecosystems in tropical and subtropical areas, accounting for more
41   than 137,760 km^2 of the world's coastline, with one of the largest areas being the Brazilian coast
42   (Spalding et al. 2010; Giri et al. 2011). These ecosystems are recognized to be of strategic importance for
43   climate change mitigation, due to their large capacity for carbon sequestration and storage, as well as for
44   protecting the coast from erosion and rising sea levels (Howard et al. 2017; Macreadie et al. 2019). Many
45   aspects of mangrove health and function are tied to microbial metabolic activities that play essential roles
46   in large-scale biogeochemical nutrient cycling and as such have been the subject of many genomic studies
47   (Yun, Deng, and Zhang 2017; Zhou et al. 2017; Imchen et al. 2017; Imchen et al. 2018; Marcos et al.
48   2018; Lin et al. 2019; Allard et al. 2020).
49   Globally, mangrove ecosystems are threatened by habitat degradation and loss due to
50   anthropogenic disturbances such as urbanization, industrial development and increasing population
51   densities in coastal areas (Fernandes et al. 2014; Imchen et al. 2018; Gong et al. 2019; Trevathan-Tackett
52   et al. 2019). In Brazil, where a large number of mangrove studies have been performed, numerous studies
53   have been conducted in disturbed mangroves (Andreote et al. 2012; Sanders et al. 2014; Cabral et al.
54   2016), mostly without direct comparison to undisturbed sites. Undisturbed mangrove sites have been
55   conserved within Brazil's Permanent Protection Areas, as defined by the National Council on the
56   Environment (CONAMA) through the resolution No. 303 of 2002 (CONAMA, 2002). Critically, this
57   resolution was revoked in September of 2020, thus increasing the risks of degradation of such areas in the
58   future.
59   One important Permanent Protection Area in Brazil, located in Bahia State, is the Pratigi area
60   which is characterized by the presence of small urban areas interspersed within dense Atlantic Rainforest
61   vegetation. Notably, when the Pratigi Protection Area was created in 1998, several small urban locations
62   were already present, and were integrated in the efforts for a sustainable use of the natural resources
63   (MMA, 2004). Despite the presence of these urban assemblages, the area has continuously received high
64   environmental quality indices (Lopes 2011; Ditt et al. 2013; Mascarenhas et al. 2019; Carneiro et al.
65   2021). Nevertheless, even with this high level of environmental quality across the entire area, some local
66   anthropogenic disturbance is still present, such as construction in what was a mangrove forest around the
67   city of Ituberá (Fig. 1). In this location, it is possible to observe clear signs of anthropogenic impact, such
68   as raw sewage and urban runoff, as well as the withdrawal of the native vegetation from the immediate
69   vicinity.
70   The existence of a small locus of disturbance within a largely conserved estuarine system
71   provides for an opportunity to study how human activities impact microbial populations. In this study, we
72   aimed to assess the impacts of urbanization on the surrounding mangrove area by examining the
73   prokaryotic communities of sediments and their potential functional roles in the context of the local
74   disturbance around Ituberá city, in comparison to the results of a distant and conserved spot in the same
75   estuarine system. Considering the increased risks of environmental disruption now that the protection
76   legislation has been revoked, this study provides important elements for the understanding of the
77   consequences of even light urbanization and minor human interference in a mangrove area.
78   Prokaryotes, specifically bacteria, comprise the large majority of the sediment microbiomes of
79   mangrove ecosystems in Brazil and worldwide, accounting for 94.8 to 99.2% of the microbial diversity
80   (Andreote et al. 2012; Imchen et al. 2018). Previous research conducted in Goa, India (Fernandes et al.
81   2014) and the Red Sea region (Ullah et al. 2017) found higher diversity in anthropogenically impacted
82   mangroves in comparison to conserved areas, possibly due to the higher availability of a wide variety of
83   organic and inorganic compounds, which favors the colonization of exogenous opportunistic prokaryotes

84   ultimately creating significantly distinct communities. In this study, we hypothesized that proximity to
85   urban environments and sources of constant input of domestic runoff leads to large-scale changes in
86   prokaryotic composition and functional profiles in the microbiome of mangrove sediments. Considering
87   the importance of prokaryotes in such areas, we conducted 16S rRNA gene sequencing analysis in both
88   conserved and impacted mangrove areas within the Serinhaém estuary, and measured the correlations
89   between the prokaryotic communities and environmental factors for each site. Using the taxonomic
90   abundances obtained with the analysis of the 16S rRNA, we estimated the general patterns of functional
91   potentials in these microbiomes.
92

Materials & Methods

93

Study area

94
95   The Serinhaém estuary (Fig. 1) is located within the limits of the Environmental Protection Area
96   of Pratigi in the state of Bahia, Brazil. The Pratigi Protection Area is defined as an area of sustainable use
97   aiming for the protection of remnants of the Brazilian Atlantic Forest and associated ecosystems, such as
98   restingas and mangroves, in which extractive and agricultural activities are still allowed but regulated
99   (MMA, 2004; Ribeiro et al. 2019). This estuarine region covers approximately 32 km of the Juliana River
100   basin, a riverine system that is completely inside the limits of the protected area, and flows into Camamu
101   Bay, a tropical oligotrophic estuarine system, where it meets the Atlantic Ocean. Ituberá is a relatively
102   small urban area of approximately 28,000 people (IBGE 2020) within the Pratigi APA, with a strong
103   economic focus on tourism. For the selection of collection sites we coordinated with the Organização de
104   Conservação da Terra (OCT) which manages conservation actions within the protection area of Pratigi.
105

Sampling

106
107   The two collection sites were located 9.5 kilometers distant from each other. The mangrove trees
108   at both collection sites are composed of the species *Rhizophora mangle*, *Avicennia schaueriana* and
109   *Laguncularia racemosa* (MDMA, 2010). Collections were performed at the morning low tide. For both
110   sites, cores consisting of the top 10 cm of the surface layer were collected using a stainless-steel
111   cylindrical sediment core sampler with a diameter of 10 cm, always avoiding mangrove trees and
112   rhizosphere associated sediments (de Santana et al. 2021).
113   At the conserved mangrove site (13°44'34.6"S, 39°03'30.6"W), collection points withing each
114   tidal zone (supralittoral, intertidal and sublittoral) were 15 m distant from each other. Within each tidal
115   zone we collected 3 sediment samples, each sample consisting of 3 combined sediment cores taken within
116   an immediate vicinity (50-60 cm), resulting in 9 samples at this site (de Santana et al. 2021). Collections
117   were made in July 2018. The conserved collection site exhibited no visible signs of anthropogenic
118   disturbance or pollution. For this study, we recombined the FASTQ files of these 9 samples into three
119   composite replicates, where each replicate included one sample from each tidal zone (Supplemental Text
120   S1).
121   The samples from the impacted site (13°44'11.1"S, 39°08'46.0"W) located just outside the city of
122   Ituberá, were collected in triplicate, each sample was located 5 m from the other two in a triangle
123   covering the sublittoral zone. As with the conserved samples, each impacted sample was composed of 3
124   sediment cores, taken within an immediate vicinity of 50-60 cm. Collections were made in February
125   2020. The definition of mangrove associated tidal zones in this area was complicated by the advance of
126   the city's construction, resulting in a smaller and partially deforested area. The emerged sediments at the
127   time of collection showed pollution by domestic runoff and construction leftovers. Because of the absence

128   of waste management infrastructure, numerous developments along the shore where the sediments were
129   taken exhibited sewage waste pipes directly releasing into the environment (Supplemental Figure S1). In
130   both collection sites the sediments from the submerged zone present a silt/mud constitution (Santos and
131   Nolasco 2017) and were collected within the tree line.
132   Sediments were transported in plastic bags inside thermic boxes filled with ice to the laboratory
133   of Petroleum Studies in the Federal University of Bahia. Samples from both sites had plants and other
134   macroscopic organic materials removed before subsequent procedures.
135   For each sediment sampling site we measured physical-chemical parameters such as dissolved
136   oxygen, conductivity, pH and temperature in the water column directly above the sampling spot of
137   submerged sediments, using a multiparameter monitoring system (YSI model 85, Columbus). For each
138   sediment core an aliquot was separated for the measurement of organic matter content using the 'loss-on-
139   ignition' method (Nelson and Sommers 1996) and the other part was kept in the -20°C freezer for DNA
140   extraction.
141   For heavy metal analysis we relied on previously performed work (Pereira 2016) which identified
142   the background metal concentrations in the sediments of the entire estuarine channel. The analysis of
143   heavy metals was carried out as described in (Pereira 2016). Briefly, 0.5 g of the clay fraction of the air-
144   dried samples were transferred to test tubes (25x25 mm) added with a solution of hydrochloric acid (HCl)
145   and nitric acid (HNO 3) at the ratio 3:1 (3 mL HCl and 1 mL HNO3) and placed in the 100 °C digester
146   block for 24 hours along with analytical blanks. After digestion, samples were filtered and placed in 50
147   ml volumetric flasks, added with ultrapure water to the extent of 25 ml and subsequently analyzed to
148   determine the concentrations of the metals Al, As, Ba, Co, Cr, Cu, Fe, Li, Mn, Ni, Pb, Sn, V, and Zn by
149   Inductively Coupled Plasma - Optical Emission Spectrometry (ICP / OES) (Agilent Technologies - 700
150   series). Data from those downstream sites closest to the sediment sampling sites (Supplemental Text S1),
151   had an average distance of 1.64 km for the impacted site and 6.98 km for the conserved site. Kruskal-
152   Wallis was performed to identify significant differences in values between the two sites (Supplemental
153   Text S1).
154
155   **DNA extraction, amplicon library generation, and sequencing**
156   Total genomic DNA was extracted using PowerSoil DNA Isolation Kit (Qiagen, Carlsbad, CA,
157   USA) from 0.25 g of each composite sample and stored at -80º C before amplification, resulting in 9
158   DNA samples for the conserved site and 3 DNA samples for the impacted site. For amplification of the
159   V4 region of the prokaryotic 16S rRNA gene we performed PCR using the primer pairs. For the
160   conserved site we used 515F-Y(Parada, Needham, and Fuhrman 2016) and 806R-XT (Caporaso et al.
161   2011), while 515F and 806R (Kozich et al. 2013) were used for the impacted samples. Each sample
162   required a minimum of 12.5 ng before PCR as quantified using Qubit (Thermo Scientific, Waltham, MA
163   USA). For PCR we used the following protocol: for 2.5 µl of each sample (minimum 5 ng/µL), 5 µl of the
164   forward and reverse primers and 12.5 µl of the 2x KAPA HiFi HotStart ReadyMix were added, to the
165   total volume of 25 µl. The samples were then subjected to following cycles: 1 x 95°C for 3 minutes, 25 x
166   95°C for 30 seconds, 1 x 55°C for 30 seconds and 1 x 72°C for 30 seconds and 1 x 72°C for 5 minutes.
167   Negative controls were also used in parallel and ran on an agarose gel, as no band resolved these were not
168   sequenced. PCR cleanup was performed using Ampure XP beads. Amplicon libraries were prepared using
169   the Nextera XT according to manufacturer's directions (Illumina, San Diego, CA, USA). Final
170   quantification and pooling were performed using KAPA HiFi. For the conserved site we loaded ~6 pM of
171   each sample for paired-end sequencing (2x150) (Caporaso et al. 2012) performed using the Illumina

172 MiSeq platform (Illumina, San Diego, CA, USA), V2 kit (300 cycles), while the impacted site we used
173 ~48 pM of each sample for paired-end sequencing (2x250) using the Illumina NovaSeq XP (Illumina, San
174 Diego, CA, USA). It is possible that these methodological differences in library preparation and
175 sequencing may produce artifactual differences in the two data sets.**Data analysis**

176 **Read preprocessing**
177   Demultiplexed sequences were filtered and trimmed with Trimmomatic (Bolger, Lohse, and
178 Usadel 2014) (ILLUMINACLIP:TruSeq3-PE.fa:2:30:10 LEADING:3 TRAILING:3
179 SLIDINGWINDOW:4:15 MINLEN:100) with the requirement of a minimum average read quality score
180 of 15 for inclusion. For each read, the sliding window cuts any read at the point where the median quality
181 score over a 4nt window is less than 15.

182

183 **Paired-end merge, denoise, and chimera removal using DADA2**
184   Paired reads from the conserved site were combined as described previously (de Santana et al.
185 2021), briefly, paired reads were combined using QIIME2 for reads with an overlap greater than 9 while
186 paired reads with an overlap greater than 6 were combined using a custom script (Supplemental Text S1)
187 before denoising using DADA2 (denoise-single, --p-trim-left 3, --p-trunc-len 0, --p-max-ee 2.0, --p-trunc-
188 q 2). The reads from the impacted site were also denoised using DADA2 (denoise-paired, --p-trim-left-f
189 13, --p-trim-left-r 13, --p-trunc-len-f 150, --p-trunc-len-r 150). These were then merged with the denoised
190 sequences from the conserved site for further analysis. Reads were resolved and clustered into amplicon
191 sequence variants (ASVs) using QIIME2 (Bolyen et al. 2019). All ASVs were retained in the data set.
192 Filtering was performed only on taxa and only for differential abundance analysis.
193   Taxonomic assignment was performed using QIIME2's naive Bayes scikit-learn classifier
194 (Bokulich et al. 2018) trained using the 16S rRNA gene sequences in SILVA database (Silva SSU 132),
195 (McDonald et al. 2012), (Supplemental Text S1). Taxonomic counts were also used for hierarchical
196 correlation clustering (Supplemental Text S1) tests using gneiss in QIIME2.
197 Unnormalized ASV (Supplemental Table S1) and taxonomic abundances (Supplemental Table S2) as
198 well as overlap (Supplemental Text S1) between sites are reported in supplemental material.

199

200 **ASV analysis using QIIME2**
201   Alpha-rarefaction curves were generated using QIIME2 (Supplemental Text S1). We performed a
202 variety of alpha-diversity (Kruskal-Wallis statistic, and Supplemental Fig. S2) and beta-diversity tests
203 (PERMANOVA statistic, Supplemental Fig. S3). As both Kruskal-Wallis and PERMANOVA are non-
204 parametric tests we did not test for normality. However, both are sensitive to homoscedasticity. For
205 Kruskal-Wallis we used Levene's test (Df=1, F-value=0.2275, p-value = 0.6334) and betadisper
206 (Anderson 2006) for PERMANOVA (Df=1, Sum_Sq=0.002209, Mean_Sq=0.002209, F-value=0.8045,
207 p-value = 0.4205).

208

209 **Environmental variable correlations using Vegan**
210   Correlations between taxonomic community structure and environmental variables associated
211 with the sample sites were tested using the Vegan package (version 2.5-6) (Dixon 2003) in R (R Core
212 Team 2019). Distance matrices were calculated using vegfit (default settings) on taxa abundance
213 identified by QIIME2 for each site. We performed constrained ordination of the distance matrices (PCoA)
214 using envfit (default settings).

215

Potential functional analysis using PICRUSt2

216
217 We used PICRUSt2 (version 2.3.0-b) (Ye and Doak 2009; Louca and Doebeli 2018; Douglas et
218 al. 2019; Barbera et al. 2019; Czech, Barbera, and Stamatakis 2020) with default settings for functional
219 analysis using the observed ASV abundances generated by QIIME2. It is important to note that functional
220 predictions generated by PICRUSt2 using 16S rRNA sequences alone will not be as accurate as a
221 metagenome including the functional sequences themselves would be (Sun et al., 2020). Because we are
222 reliant on 16S rRNA gene all KEGG ortholog (KO) abundances are derived from the closest reference
223 taxa that matches the supplied taxa. As such there may be significant differences between the KO of the
224 actual organism and the reference we rely on.

225 To address this, we use PICRUSt2's nearest sequenced taxon index (NSTI) as a heuristic cutoff in
226 the evaluation of taxon level functional analysis (Supplemental Table S3). Although we are using
227 taxonomic families in this study, we will continue to use the NSTI cutoff of 0.15, despite it being derived
228 for species level comparisons. Where relevant, families with median NSTI scores within 1 standard
229 deviation of 0.15 are labeled with an asterisk (*). Only one family, *Pirellucae*, was both significantly
230 enriched in metabolic KOs while also having an NSTI outside of this range; this family was not included
231 in the analysis.

232 KEGG Orthologs (KOs) were subsequently analyzed for significant (p-value <= 0.05) differential
233 abundances after centered log-ratio transformation (aldex.clr) using the general-linear model method
234 (aldex.kw) of the ALDEx2 package (ver 1.18.0). These were then used for the construction of the
235 heatmaps of KOs with differential abundance between pristine and impacted mangrove. Pathway analysis
236 of these KOs was performed using KEGG Mapper (Kanehisa and Sato 2020). For a pathway to be
237 considered we required that the entire pathway needed to be significantly enriched at a single site (i.e.
238 'complete').

239

Differential abundance analysis

240
241 In order to identify which taxa were significantly different in abundance in each sampling area we
242 carried out a taxa enrichment analysis. ASV abundances were normalized by total sum scaling (TSS)
243 wherein each ASV read abundance is reduced by a fraction so that the total sample is downsampled to
244 match the least abundant sample in the experiment (Weiss et al. 2017). ASVs were combined into
245 assigned taxa using the taxonomic results of QIIME2. To be defined as significantly different, several
246 criteria must be met: there must be at least 100 unnormalized counts of the taxa in at least one site, the
247 sets of observations between sites must be statistically significant (p-val <= 0.05) as calculated using the
248 Kruskal-Wallis H test and finally, the effect size must be in excess of a 20% difference in abundance
249 between sites.

250 Since TSS normalization can confound interpretation, we also applied the same method to data
251 that had been normalized using cumulative sum scaling (CSS). CSS is a normalization approach that
252 weights the normalization factor based on the relative abundance of ASVs against the total abundance
253 (Paulson et al. 2013). However, as we observed that this approach resulted in the loss of several common
254 taxa and the gain of many more marginal taxa (Supplemental text S1) we chose to use the TSS
255 normalization method.

256 A further extension of differential abundance is to identify taxa which are exclusive to a single
257 site. In order to determine taxa exclusive to a single site with a high degree of certainty we required a
258 taxon to have been observed 0 times (using unnormalized abundances) at one site and at least 100 counts
259 at the other, with a minimum of 10 counts per replicate.

260 Gneiss hierarchical clustering is an alternative approach that uses balance calculations to extend
261 differential abundance analysis beyond species and instead identify niche specific subcommunities
262 (Morton et al. 2017). Using this approach hundreds of taxa were found to be differentially abundant
263 between the two sites (Supplemental Text S1) with all but 3 of our predicted differentially abundant taxa
264 being present in the appropriate enriched cluster.
265
266 **Taxa specific predicted contribution to metabolic pathway functional abundances**
267 We calculated metabolic pathway enrichment specific to a given taxa at a given taxonomic level.
268 For this we relied on the predicted relative functional abundance results of PICRUSt2. First, for each
269 taxon, at each level, we combined all predicted relative functional abundances of KOs belonging to
270 certain metabolic pathways: methane (ko00680), nitrogen (ko00910), sulfur (ko00920), and pentose
271 phosphate (ko00030) metabolism - as well as, carbon fixation pathways in prokaryote (ko00720), carbon
272 fixation pathways in photosynthetic organisms (ko00710), and photosynthesis (ko00195). We then
273 applied Kruskal-Wallis H test to identify taxa that had significantly different taxa-specific pathway
274 abundances. Furthermore, we require that a taxon at a single site must be significantly enriched relative to
275 the other sites and that the taxa contributes at least 5% of the total relative functional abundance in at least
276 one site.
277
278 The entire computational workflow is available as a repository in GitHub:
279 https://github.com/pspealman/Project_Impact.
280
281 The impacted mangrove sediment sequencing data is available from NCBI BioProject PRJNA650560,
282 while the pristine mangrove sediment data is available from NCBI BioProject as accession number
283 PRJNA608697.
284

285 # Results
286 **Structural aspects of prokaryotic communities of mangrove sediments**
287 Taxonomic assignment of the prokaryotes in the mangrove samples resulted in a total of 7,278
288 ASVs (Supplemental Table S1), belonging to 1,369 taxa (Supplemental Table S2), 861 of which had at
289 least 20 unnormalized reads in at least one site (Supplemental Text S1). These resolved to 184 taxa at the
290 family level or higher, with 124 having at least 20 unnormalized reads at a single site. 60 (48%) of these
291 were present at both sites, while 13 (11%) were unique to the conserved site, and 51 (41%) were unique
292 to the impacted site (Supplemental Text S1). Bacteria accounted for nearly 91% of all reads while
293 archaeal taxa accounted for 7.9% and unassigned groups only 1.6%. The two mangrove areas presented
294 considerable differences at the phylum level for the 12 most abundant phyla. Figure 2 displays all the
295 classes belonging to the top 12 phyla with more than 1% abundance in the analysis. Some phyla such as
296 Firmicutes and Planctomycetes presented a large decrease in abundance in the impacted site when
297 compared to the conserved site, while the presence of the entire phylum Euryarchaeota was only detected
298 in the urbanized mangrove (Fig. 2). Some phyla were represented by different Classes in each site, as is
299 the case of Chloroflexi, with *Dehalococcoidia* only prevailing in the impacted mangrove site. Below the
300 family level we observed a dominance of unassigned groups (Supplemental Text S1).
301 The analysis revealed significantly higher richness (Total ASVs, Kruskal-Wallis H = 3.857, df =
302 1, p-value = 0.050) and diversity (Shannon's diversity, Kruskal-Wallis H = 3.857, df = 1, p-value =
303 0.050) in the impacted mangrove sediments (Fig. 3A and 3B), relative to the conserved sediments.

304 Additional alpha-diversity test results are available in Supplemental Text S1. Prokaryotic community
305 composition differed between the two sites with marginal significance (PERMANOVA, permutations =
306 999, pseudo-F = 3.285, p-value = 0.096), (see Supplemental Text S1 for additional beta-diversity tests)
307 (Fig. 3C). Samples of each mangrove site form separate clusters as can be seen in the PCoA plot (Fig.
308 3D). The PCoA plot also shows that the samples from the conserved mangrove site present higher
309 variability than the samples collected at the impacted site. The results showed a significant (p-value <=
310 0.05) correlation between the structure of prokaryotic communities and some environmental variables
311 (Supplemental Text S1). These include organic matter (conserved site mean: 3.8%, impacted site mean:
312 9.9%), temperature (27.7°C, 29.3°C), and Cu (0 mg Kg^{-1}, 0.16 mg Kg^{-1}). While dissolved oxygen (5.54 mg
313 L^{-1}, 8.21 mg L^{-1}), pH (7.62, 7.46), Ba (0.66 mg Kg^{-1}, 0.44 mg Kg^{-1}), and salinity (15.1 ppt, 13.3 ppt) were
314 only marginally significant (p-value <= 0.1) (Fig. 3D).
315   The majority of families with significant (p < 0.05) differences in abundances between sites were
316 found in the sediments of the impacted mangrove. Figure 4 shows the 64 families with significant and
317 large effect size differences between the sites (>20%) and those that are absent in one of the areas. We
318 found 35 families that had significantly higher abundance in the impacted mangrove site, including
319 human associated and human pathogen associated families *Burkholderiaceae* (Coenye 2014),
320 *Pasteurellaceae*, *Spirochaetaceae*, *Ruminococcaceae*, *Veillonellaceae*, and *Rikenellaceae*. Also more
321 prevalent in the impacted sediment were known archaeal methanogens *Methanomicrobia* and
322 *Thermoplasmata* (Whitman, Bowen, and Boone 2014), Fe and Mn metabolizing *Geobacteraceae* (Röling
323 2014), and members of *Gammaproteobacteria* associated with sulfur metabolism *Syntrophobacteraceae*
324 (Liu and Conrad 2017), *Thioalkalispiraceae* (Mori and Suzuki 2014), *Saccharospirillaceae* (Vavourakis
325 et al. 2019), *Thiomicrospiraceae* (Eberhard et al. 1995); methanogen *Methylomonaceae* and nitrogen
326 metabolising *Nitrincolaceae*. We also found *Lachnospiraceae* and *Anaerolineae* members of which were
327 found to be of greater abundance in PVC contaminated environments (Seeley et al. 2020).
328   We also found 9 families with higher abundance in the conserved sediments. These include
329 *Thermoanaerobaculaceae*, recently shown to have a high metabolic diversity in wastewater treatment
330 plants (Kristensen et al. 2021), which along with *Pirellulaceae*, was recently found to be sensitive to
331 microplastic pollution (Seeley et al. 2020). All enriched members of Planctomycetes, some of which are
332 capable of anaerobic ammonia oxidation (anammox) have greater abundance at the conserved site, except
333 MSBL9 SG8-4, potentially because of its freshwater preference (Andrei et al. 2019). We also observed
334 the pathogen associated *Vibrionaceae* (Farmer 2006) in the area.
335
336 **Functional aspects of prokaryotic communities of mangrove sediment**
337   Functional profiles of the prokaryotic communities generated with PICRUSt2 based on the
338 taxonomic abundances allowed us to identify statistically different potentials for carbon, nitrogen,
339 phosphorus and sulfur metabolic pathways between the conserved and impacted mangrove sites (Fig. 5
340 and 6).
341   The carbon metabolism heatmaps are subdivided in: carbon fixation for photosynthetic organisms
342 (ko00710), prokaryotes (ko00720) and methane (ko00680) metabolism, in order to allow a better
343 visualization (Fig. 5). Generally, the methane and carbon fixation pathways presented higher functional
344 abundance in the impacted site than that of the conserved mangrove. We found that the impacted site is
345 enriched in the formaldehyde assimilation pathway (M00345), methane metabolism modules, (M00563)
346 Methanogenesis, 2-Oxocarboxylic acid chain extension (M00608), light Crassulacean acid metabolism
347 carbon fixation (M00169), and Serine biosynthesis (M00020).

348   The nitrogen metabolism heatmap (Fig. 6) presents enrichment of metabolic pathways in the
349   impacted mangrove site, with a significant enrichment in the nitrogen to ammonia fixation module
350   (M00175). The functional profile of pentose phosphate metabolism also shows a tendency for enrichment
351   of KOs in the impacted mangrove area. This enrichment includes the pentose phosphate pathway
352   (M00004), PRPP biosynthesis (M00005), both oxidative (M00006) and non-oxidative phases (M00007),
353   the Entner-Doudoroff pathway (M00008), as well as the archaeal pathway (M00580). For sulfur
354   metabolism, we found that some KOs are absent or nearly absent in the conserved sediments while
355   generally present in the impacted area. In the conserved area, we found significant enrichment only in the
356   cysteine biosynthesis (M00021) pathway. While photosynthesis associated KOs were relatively low, we
357   did find significant enrichment in the conserved sediment for both photosystems I (M00163) and II
358   (M00161), we also found that the impacted site is significantly enriched in F-type ATPase ATP synthesis
359   (M00157). Taken together, these findings suggest that the high abundance and diversity in the impacted
360   area leads to enrichment in several metabolic pathways, including several wholly absent from the
361   conserved area.
362   We also analyzed the contribution each family makes to the metabolism of the elements C, N, P
363   and S. Families that contribute 5% or more to a given nutrient cycle in at least one site are represented in
364   Fig. 7. We found the majority of the families with large contributions to the metabolic pathways in the
365   conserved mangrove sediments, which display the lower biodiversity. The families *Bacillaceae* and
366   *Stappiaceae* were greatly important for nutrient metabolism in the conserved mangrove sediments but not
367   in the impacted sediments. Conversely, only *Syntrophaceae*, and *Desulfarculaceae* presented large
368   functional contributions for the impacted mangrove area. *Anaerolineaceae* and *Desulfobacteraceae*
369   showed important contributions for the functional potentials in both studied areas. This is consistent with
370   a lower biodiversity leading to a higher number of taxa making larger contributions to the total functional
371   potential.
372
373   **Discussion**
374   Anthropogenic impacts are known to cause important changes both in structure and function of
375   sediment microbiomes in mangroves (Ottoni et al. 2017; Imchen et al. 2018; Allard et al. 2020). In our
376   study, we observed biodiversity to be higher in the impacted mangrove sediments than at the conserved
377   site. Similar observations have been made previously in the comparison between conserved and
378   anthropized mangrove areas in India (Fernandes et al. 2014) and the Red Sea region (Ullah et al. 2017).
379   Here we find that organic matter is one of the most significant drivers of prokaryotic structuring between
380   the measured environmental variables (Fig. 3). The large differences in organic matter contents could be
381   the product of the urban runoff at the impacted site, which presented higher levels (median OM 9.9%) in
382   comparison with the conserved area (median OM 3.8%). This suggests that this environment may have
383   become more eutrophic due to the constant exposure to urban tailings, as observed *in locu*, which results
384   in greater biomass production and biodiversity (Fernandes et al. 2014; Glibert 2017). While some studies
385   that use incubation or microcosm approaches have observed decreasing microbial diversity as a result of
386   nutrient addition, in experiments with coastal soils (Aoyagi et al 2015; Wang et al 2016; Bulseco et al
387   2019; Craig et al 2021), our study relied on field sediments which are continually exposed to
388   anthropogenic presence, as such, would be expected to differ from controlled microcosms.
389   Besides organic matter, the structure of the prokaryotic communities in these mangrove
390   sediments was greatly influenced by other environmental factors, such as temperature, copper content,
391   pH, salinity and barium concentrations (Fig. 3D). Some of these, such as salinity and pH are the result of

392   naturally driven biogeochemical processes in the area, while others, such as metal content, were observed
393   to reflect the natural lithology of the estuary area (Pereira 2016) or tidal deposition, as is the case with Ba
394   (Carneiro et al. 2021).
395   Beyond the presence of an urban complex, other differences exist between the two sites as they
396   are located along a gradient from river source to ocean. Notably, the increasing salinity due to proximity
397   to the sea can impair the bioavailability of organic matter in these sediments, consequently affecting the
398   availability of nutrients (Filippino et al. 2011). The different sources of dissolved and particulate OM in
399   aquatic environments also have large effects on the contents, species, and availability of nutrients such as
400   N, P, and heavy metals (Dong et al. 2020). Although mangrove species show an optimal growth over a
401   large range of salinity (Krauss 2008), and the differences observed in this study are small, all these factors
402   may interact synergistically with the observed anthropogenic impacts, such as deforestation and
403   construction byproducts, as well as urban tailings, to create a completely different sediment environment.
404   We sought to identify differences in the metabolic systems of the two sites using functional
405   profiling. However, the functional profiles were not obtained by metagenomic sequencing, but based on
406   the abundances of identified taxa compared to a reference holotype. To highlight this important limitation,
407   we refer to these functional profiles as potential metabolic abundances. Although the use of metagenomic
408   sequencing can provide better resolution to functional profiling (Zhang et al., 2021), it is possible to
409   recover the general patterns of the microbiome functions through the taxonomic abundances of the 16S
410   rRNA genes (Jovel et al., 2016). The diversity of taxa contributing to the metabolic pathways of the
411   studied nutrient cycles is in accordance with the premise that soil and sediment microbial communities
412   present elevated functional versatility (Barnes, Carter, and Lewis 2020), where many taxonomic groups
413   can play considerable roles in a variety of functions.
414   We observed that the potential functional abundance for the metabolism of specific elements
415   were spread across taxa as a function of biodiversity. Specifically, the impacted site, with a higher
416   number of taxonomic groups, had fewer taxa making large contributions (>5%) to the metabolic
417   potentials, while the conserved site with low diversity showed a higher number of families contributing
418   greatly to such metabolisms. Some taxa, such as *Desulfobacterales*, an important sulfate-reducing
419   bacteria, have been previously shown to contribute greatly with important nutrient metabolisms in
420   mangrove sediments (Ullah et al. 2017; Nie et al. 2021). This is in accordance with our results where the
421   *Desulfobacterales* taxa was also an important contributor to carbon and nitrogen metabolisms in both
422   mangrove areas (Fig. 7). Taken together the results support the conclusion that, the lower the biodiversity,
423   the higher the importance of particular groups to the nutrient cycles.
424   Considering that the conserved site shows that a large portion of the ecosystem function is
425   dependent on a small number of taxa and that large differences exist between the taxa of the two sites, it
426   may be expected that the urbanization process and the subsequent disturbance in the microbiome
427   population would lead to an imbalance in nutrient cycling, potentially impairing some important
428   metabolisms. The analysis of functional profiles suggests, however, the opposite trend where the
429   functional potentials for these metabolisms are higher in the impacted mangrove site. Despite this
430   increased metabolic activity at the impacted site, the ultimate effect these changes have on metabolic
431   output, such as carbon sequestration or methane production, is difficult to predict. Previous work has
432   shown that the increased consumption of carbon may not lead to increased sequestration as increased
433   decomposition may lead to lower carbon burial rates (Bulseco 2019).
434   Furthermore, the potential maintenance of the KOs and modules that make up nutrient cycles is
435   not a guarantee of a healthy ecosystem. Changes in nutrient availability caused by human interference

436   have previously been shown to affect the diversity of sulfate-reducing (SRB) and sulfur-oxidizing
437   bacteria (SOB) (Meyer et al. 2016), thus interfering in the cycling of this element. Indeed, we see
438   numerous prokaryotic species negatively affected by human impacts and there is great potential for
439   eukaryotic species to be impacted as well. The alteration in microbiome nutrient cycling driven by
440   urbanization is potentially hazardous as it can increase primary production, leading to a higher spatial and
441   temporal hypoxia in the aquatic environment (Houser and Richardson 2010), resulting in a cascading
442   effect in the system. Although Camamu Bay is a well conserved coastal system, it does contain low
443   abundances of toxic cyanobacteria, such as *Microcystis*, that have the potential to form blooms in
444   eutrophic waters, which, in turn, is consistent with habitat degradation trends reported in estuaries
445   worldwide (Affe et al. 2018).
446   In this work we found widespread variance in taxa abundance between sites up to and including
447   the possible extinction of families at the impacted site (Fig. 4). Although the majority of taxa observed at
448   the conserved site persisted in the impacted site, some families could be identified only in the conserved
449   sediments. Here, we consider the absence of groups in the impacted site as indicative of a possible local
450   extinction caused by human interference. The absences of some families are consistent with local
451   extinction driven by anthropogenic change, such as subgroup 9 of *Acidobacteria*, which despite having a
452   relatively high abundance at the conserved site is entirely absent from the impacted site. Notably many
453   members of this taxa are known to be oligotrophic with a strong negative correlation with the organic
454   carbon in the environment (Kielak et al. 2016). Conversely, for some families, such as *Caldilineaceae* and
455   *Rubritaleaceae,* whose ecological aspects are still not well documented, their absence in the impacted
456   mangrove suggests that these groups could also be oligotrophic or sensitive to some components of urban
457   pollution, warranting further studies.
458   Similarly, some of the taxa that were enriched or unique for the impacted mangrove area could be
459   directly correlated with the discharge of domestic sewage in the area. The prevalence of the family
460   *Pasteurellaceae* is an example, since most of its subgroups are known pathogens of vertebrates and are
461   not usually found outside hosts (Christensen et al. 2014). Additionally, many genera belonging to the
462   family *Spirochaetaceae* are known for causing a variety of human diseases such as syphilis, Lyme
463   disease, leptospirosis, and periodontal disease, among others (Karami et al. 2014). Furthermore, members
464   of the *Ruminococcaceae* are among the most abundant groups found in the mammalian gut environment
465   (Biddle et al. 2013). *Veillonellaceae* is a diverse family with varying degrees of antimicrobial resistance
466   and is associated with disease in both animals and humans (Marchandin and Jumas-Bilak 2014). Finally,
467   the enrichment in the *Rikenellaceae* family could be further evidence of fecal contamination, as the
468   presence of subgroups of *Bacteroidales* has been proposed as a predictor of the risk of waterborne
469   diseases (Schriewer et al. 2010).
470   In addition to the concerns about the prevalence of known human and animal pathogenic groups,
471   recent studies have also shown the dissemination of antibiotic resistance genes in diverse mangrove
472   compartments, including the sediment-root continuum, with antibiotic resistance sorting independently of
473   the associate microbiota (Wang et al. 2021; Imchen and Kumavath 2021). Antibiotic resistance itself is
474   highly correlated with anthropogenic interference in mangroves, which is in turn strongly determined by
475   local socioeconomic factors (Imchen and Kumavath 2021). In this sense, the anthropogenic impacts in
476   mangrove ecosystems can lead to consequences beyond the ecosystem threats and health risks for the
477   local human population, but it can potentially increase global health threats with the spread of antibiotic
478   resistance in pathogenic microbes.

479   We also observed that the variance in communities between replicates was greater in the
480   conserved samples. While this could represent higher diversity in conserved microbiomes, other factors
481   could potentially play a role. Importantly sample collection at the conserved site spanned a larger distance
482   with 15 m instead of 5 m separating the sample sites, and there was a more pronounced separation of tidal
483   zones as well. The small number of samples is also a relevant limitation, especially for matters of
484   statistical analysis. Additionally, the two sites, although sharing the same watershed and estuary, were
485   ~10 Km apart, and as such, numerous environmental differences may contribute to the variance as well.
486   Nevertheless, the largest difference observed in physical parameters was the presence/absence of
487   urbanization at the site. Considering that the samples from the impacted area were collected nearby
488   domestic runoff sources, while the conserved site presented no signs of anthropogenic impact, and that
489   some of the taxa uniquely found in the impacted sediments are recognized as pathogenic and gut
490   microbiome colonizers, we consider that these important differences are correlated with the observed
491   human impacts.
492   Our results show that the microbial communities of sediments can be largely affected by land use
493   in mangrove adjacent areas, and that the observation of some particular prokaryotic groups are potential
494   bioindicators of such human impacts, as well as posing risks to the surrounding populations. Notably,
495   Brazilian mangroves are currently under elevated risk due to recent changes in the environmental
496   legislation in the nation. Therefore, decision making organizations should be aware of the sensitivity of
497   the microbiomes in this ecosystem, which play such important roles in the larger biogeochemical cycles,
498   thus affecting global nutrient cycling, and act towards the conservation of the mangroves.
499

Conclusions

501   Our study looked at the effects of urbanization on the prokaryotic communities of mangrove
502   sediments, through a comparison of samples taken from both impacted and conserved areas of the same
503   estuarine system. The analysis found a statistically relevant change in the structure of the communities
504   and an elevation of prokaryotic biodiversity in the sediments of the urbanized mangrove area. The
505   predicted functional analysis showed that the general patterns of nutrient metabolisms could be
506   maintained and that the metabolic potentials in the impacted mangrove were higher than in conserved
507   mangroves, likely due to the higher biodiversity present in the impacted area. The observation of diverse
508   groups contributing to metabolic pathways suggests higher versatility in the impacted mangrove
509   sediments, where the functions are carried out by a greater number of groups, while fewer groups are
510   responsible for large functional contributions in the conserved site. Beyond the differing nature of the
511   sources of organic compounds and clear physical impacts between the areas, other environmental factors
512   also played a significant role in the structure of the microbial communities. Notably, some of these may
513   act synergistically to create the different patterns observed. Despite increasing biodiversity on the
514   mangrove ecosystem, the presence of an urban settlement showed some clear negative effects, such as the
515   extinction of some prokaryotic groups, as well as the colonization by human and animal pathogens in the
516   microbiome of the impacted area. In this sense, the relative stability observed in functional terms does not
517   imply the absence of a negative impact and recent studies confirm that human interference can lead to the
518   spread of antibiotic resistance in mangrove sediments, which can cause serious health issues globally.
519   This study provides evidence that the impacts of urbanization are reflected also in microbiological scales
520   inducing important changes in ecosystem functions that could, in turn, impact the biogeochemical cycles
521   in larger scales if not monitored and controlled. Future microbiome studies should be expanded to include
522   eukaryotes, fungi, and viruses for a more complete profile of the microbial populations in these areas.

523 Direct measurements of carbon, contaminants, and nutrient cycling rates in the field would also be
524 valuable to verify the functional profiling results obtained in this work.
525

526 Acknowledgements

527 The authors would like to thank the Organização de Conservação da Terra (OCT) for providing the
528 structure for the field work in the environmental protection area, and the sequencing facility of the
529 Microbial Ecology and Biotechnology Laboratory (LEMBiotec).

530

531 References

532 Affe HM de J, Rigonato J, Nunes JM de C, Menezes M. 2018. Metagenomic Analysis of Cyanobacteria
533   in an Oligotrophic Tropical Estuary, South Atlantic. *Frontiers in microbiology* 9:1393. DOI:
534   10.3389/fmicb.2018.01393.
535 Allard SM, Costa MT, Bulseco AN, Helfer V, Wilkins LGE, Hassenrück C, Zengler K, Zimmer M, Erazo
536   N, Mazza Rodrigues JL, Duke N, Melo VMM, Vanwonterghem I, Junca H, Makonde HM, Jiménez
537   DJ, Tavares TCL, Fusi M, Daffonchio D, Duarte CM, Peixoto RS, Rosado AS, Gilbert JA, Bowman
538   J. 2020. Introducing the Mangrove Microbiome Initiative: Identifying Microbial Research Priorities
539   and Approaches To Better Understand, Protect, and Rehabilitate Mangrove Ecosystems. *mSystems* 5.
540   DOI: 10.1128/msystems.00658-20.
541 Anderson MJ. 2006. Distance-based tests for homogeneity of multivariate dispersions. *Biometrics*
542   62:245–253. DOI: 10.1111/j.1541-0420.2005.00440.x.
543 Andrei A-Ş, Salcher MM, Mehrshad M, Rychtecký P, Znachor P, Ghai R. 2019. Niche-directed evolution
544   modulates genome architecture in freshwater Planctomycetes. *The ISME journal* 13:1056–1071. DOI:
545   10.1038/s41396-018-0332-5.
546 Andreote FD, Jiménez DJ, Chaves D, Dias ACF, Luvizotto DM, Dini-Andreote F, Fasanella CC, Lopez
547   MV, Baena S, Taketani RG, de Melo IS. 2012. The microbiome of Brazilian mangrove sediments as
548   revealed by metagenomics. *PloS one* 7:e38600. DOI: 10.1371/journal.pone.0038600.
549 Aoyagi T, Kimura M, Yamada N, Navarro RR, Itoh H, Ogata A, Sakoda A, Katayama Y, Takasaki M,
550   Hori T. 2015. Dynamic transition of chemolithotrophic sulfur-oxidizing bacteria in response to
551   amendment with nitrate in deposited marine sediments. Frontiers in microbiology 6:426. DOI:
552   10.3389/fmicb.2015.00426.
553 Barbera P, Kozlov AM, Czech L, Morel B, Darriba D, Flouri T, Stamatakis A. 2019. EPA-ng: Massively
554   Parallel Evolutionary Placement of Genetic Sequences. *Systematic biology* 68:365–369. DOI:
555   10.1093/sysbio/syy054.
556 Barnes EM, Carter EL, Lewis JD. 2020. Predicting Microbiome Function Across Space Is Confounded by
557   Strain-Level Differences and Functional Redundancy Across Taxa. *Frontiers in microbiology* 11:101.
558   DOI: 10.3389/fmicb.2020.00101.
559 Biddle A, Stewart L, Blanchard J, Leschine S. 2013. Untangling the Genetic Basis of Fibrolytic
560   Specialization by Lachnospiraceae and Ruminococcaceae in Diverse Gut Communities. *Diversity*
561   5:627–640. DOI: 10.3390/d5030627.
562 Bokulich NA, Kaehler BD, Rideout JR, Dillon M, Bolyen E, Knight R, Huttley GA, Gregory Caporaso J.
563   2018. Optimizing taxonomic classification of marker-gene amplicon sequences with QIIME 2's q2-
564   feature-classifier plugin. *Microbiome* 6:90. DOI: 10.1186/s40168-018-0470-z.

565 Bolger AM, Lohse M, Usadel B. 2014. Trimmomatic: a flexible trimmer for Illumina sequence data.
566   *Bioinformatics* 30:2114–2120. DOI: 10.1093/bioinformatics/btu170.
567 Bolyen E, Rideout JR, Dillon MR, Bokulich NA, Abnet CC, Al-Ghalith GA, Alexander H, Alm EJ,
568   Arumugam M, Asnicar F, Bai Y, Bisanz JE, Bittinger K, Brejnrod A, Brislawn CJ, Brown CT,
569   Callahan BJ, Caraballo-Rodríguez AM, Chase J, Cope EK, Da Silva R, Diener C, Dorrestein PC,
570   Douglas GM, Durall DM, Duvallet C, Edwardson CF, Ernst M, Estaki M, Fouquier J, Gauglitz JM,
571   Gibbons SM, Gibson DL, Gonzalez A, Gorlick K, Guo J, Hillmann B, Holmes S, Holste H,
572   Huttenhower C, Huttley GA, Janssen S, Jarmusch AK, Jiang L, Kaehler BD, Kang KB, Keefe CR,
573   Keim P, Kelley ST, Knights D, Koester I, Kosciolek T, Kreps J, Langille MGI, Lee J, Ley R, Liu Y-
574   X, Loftfield E, Lozupone C, Maher M, Marotz C, Martin BD, McDonald D, McIver LJ, Melnik AV,
575   Metcalf JL, Morgan SC, Morton JT, Naimey AT, Navas-Molina JA, Nothias LF, Orchanian SB,
576   Pearson T, Peoples SL, Petras D, Preuss ML, Pruesse E, Rasmussen LB, Rivers A, Robeson MS 2nd,
577   Rosenthal P, Segata N, Shaffer M, Shiffer A, Sinha R, Song SJ, Spear JR, Swafford AD, Thompson
578   LR, Torres PJ, Trinh P, Tripathi A, Turnbaugh PJ, Ul-Hasan S, van der Hooft JJJ, Vargas F,
579   Vázquez-Baeza Y, Vogtmann E, von Hippel M, Walters W, Wan Y, Wang M, Warren J, Weber KC,
580   Williamson CHD, Willis AD, Xu ZZ, Zaneveld JR, Zhang Y, Zhu Q, Knight R, Caporaso JG. 2019.
581   Reproducible, interactive, scalable and extensible microbiome data science using QIIME 2. *Nature
582   biotechnology* 37:852–857. DOI: 10.1038/s41587-019-0209-9.
583 Bulseco AN, Giblin AE, Tucker J, Murphy AE, Sanderman J, Hiller-Bittrolff K, Bowen JL. 2019. Nitrate
584   addition stimulates microbial decomposition of organic matter in salt marsh sediments. *Global
585   Change Biology* 25:3224–3241. DOI: 10.1111/gcb.14726.
586 Cabral L, Júnior GVL, Pereira de Sousa ST, Dias ACF, Lira Cadete L, Andreote FD, Hess M, de Oliveira
587   VM. 2016. Anthropogenic impact on mangrove sediments triggers differential responses in the heavy
588   metals and antibiotic resistomes of microbial communities. *Environmental Pollution* 216:460–469.
589   DOI: 10.1016/j.envpol.2016.05.078.
590 Caporaso J, Lauber CL, Walters WA, Berg-Lyons D, Huntley J, Fierer N, Owens SM, Betley J, Fraser L,
591   Bauer M, Gormley N, Gilbert JA, Smith G, Knight R. 2012. Ultra-high-throughput microbial
592   community analysis on the Illumina HiSeq and MiSeq platforms. *The ISME journal* 6:1621–1624.
593   DOI: 10.1038/ismej.2012.8.
594 Caporaso JG, Lauber CL, Walters WA, Berg-Lyons D, Lozupone CA, Turnbaugh PJ, Fierer N, Knight R.
595   2011. Global patterns of 16S rRNA diversity at a depth of millions of sequences per sample.
596   *Proceedings of the National Academy of Sciences of the United States of America* 108 Suppl 1:4516–
597   4522. DOI: 10.1073/pnas.1000080107.
598 Carneiro LM, Dourado GB, de Carvalho CEV, da Silva Júnior JB, de Jesus TB, Hadlich GM. 2021.
599   Evaluation of the concentrations of elements at trace level in the Serinhaem River estuary, Bahia,
600   Brazil, using chemometric tools. *Marine pollution bulletin* 163:111953. DOI:
601   10.1016/j.marpolbul.2020.111953.
602 Christensen H, Kuhnert P, Nørskov-Lauritsen N, Planet PJ, Bisgaard M. 2014. The Family
603   Pasteurellaceae. *The Prokaryotes*:535–564. DOI: 10.1007/978-3-642-38922-1_224.
604 Coenye T. 2014. The Family Burkholderiaceae. In: Rosenberg E, DeLong EF, Lory S, Stackebrandt E,
605   Thompson F eds. *The Prokaryotes: Alphaproteobacteria and Betaproteobacteria*. Berlin, Heidelberg:
606   Springer Berlin Heidelberg, 759–776. DOI: 10.1007/978-3-642-30197-1_239.
607 CONAMA. Conselho Nacional de Meio Ambiente. 2002. Resolução CONAMA nº. 303, de 20 de março
608   de 2002.

609 Craig H, Antwis RE, Cordero I, Ashworth D, Robinson CH, Osborne TZ, Bardgett RD, Rowntree JK,
610   Simpson LT. 2021. Nitrogen addition alters composition, diversity, and functioning of microbial
611   communities in mangrove soils: An incubation experiment. *Soil biology & biochemistry* 153:108076.
612   DOI: 10.1016/j.soilbio.2020.108076.
613 Czech L, Barbera P, Stamatakis A. 2020. Genesis and Gappa: processing, analyzing and visualizing
614   phylogenetic (placement) data. *Bioinformatics* . DOI: 10.1093/bioinformatics/btaa070.
615 Ditt E, Zysman N, Cunha RS da, Rocha RB da. 2013. Conservação Da Biodiversidade Por Meio Da
616   Atividade Extrativista Em Comunidades Quilombolas. *Revista Brasileira de Ciências Ambientais* 27.
617 Dixon P. 2003. VEGAN, a package of R functions for community ecology. *Journal of Vegetation Science*
618   14:927. DOI: 10.1658/1100-9233(2003)014[0927:vaporf]2.0.co;2.
619 Dong Y, Li Y, Kong F, Zhang J, Xi M. 2020. Source, structural characteristics and ecological indication
620   of dissolved organic matter extracted from sediments in the primary tributaries of the Dagu River.
621   *Ecological Indicators* 109:105776. DOI: 10.1016/j.ecolind.2019.105776.
622 Douglas GM, Maffei VJ, Zaneveld J, Yurgel SN, Brown JR, Taylor CM, Huttenhower C, Langille MGI.
623   2019. PICRUSt2: An improved and extensible approach for metagenome inference.
624   *Bioinformatics*:497.
625 Eberhard C, Wirsen CO, Jannasch HW. 1995. Oxidation of polymetal sulfides by chemolithoautotrophic
626   bacteria from deep-sea hydrothermal vents. *Geomicrobiology journal* 13:145–164. DOI:
627   10.1080/01490459509378014.
628 Farmer JJ. 2006. The Family Vibrionaceae. In: Dworkin M, Falkow S, Rosenberg E, Schleifer K-H,
629   Stackebrandt E eds. *The Prokaryotes: A Handbook on the Biology of Bacteria Volume 6:*
630   *Proteobacteria: Gamma Subclass*. New York, NY: Springer New York, 495–507. DOI: 10.1007/0-
631   387-30746-X_17.
632 Fernandes SO, Kirchman DL, Michotey VD, Bonin PC, LokaBharathi PA. 2014. Bacterial diversity in
633   relatively pristine and anthropogenically-influenced mangrove ecosystems (Goa, India). *Brazilian*
634   *journal of microbiology: [publication of the Brazilian Society for Microbiology]* 45:1161–1171. DOI:
635   10.1590/s1517-83822014000400006.
636 Filippino KC, Mulholland MR, Bernhardt PW, Boneillo GE, Morse RE, Semcheski M, Marshall H, Love
637   NG, Roberts Q, Bronk DA. 2011. The bioavailability of effluent-derived organic nitrogen along an
638   estuarine salinity gradient. *Estuaries and coasts: journal of the Estuarine Research Federation*
639   34:269–280. DOI: 10.1007/s12237-010-9314-1.
640 Giri C, Ochieng E, Tieszen LL, Zhu Z, Singh A, Loveland T, Masek J, Duke N. 2011. Status and
641   distribution of mangrove forests of the world using earth observation satellite data. *Global ecology*
642   *and biogeography: a journal of macroecology* 20:154–159. DOI: 10.1111/j.1466-8238.2010.00584.x.
643 Glibert PM. 2017. Eutrophication, harmful algae and biodiversity - Challenging paradigms in a world of
644   complex nutrient changes. *Marine pollution bulletin* 124:591–606. DOI:
645   10.1016/j.marpolbul.2017.04.027.
646 Gong B, Cao H, Peng C, Perčulija V, Tong G, Fang H, Wei X, Ouyang S. 2019. High-throughput
647   sequencing and analysis of microbial communities in the mangrove swamps along the coast of Beibu
648   Gulf in Guangxi, China. *Scientific reports* 9:9377. DOI: 10.1038/s41598-019-45804-w.
649 Houser JN, Richardson WB. 2010. Nitrogen and phosphorus in the Upper Mississippi River: transport,
650   processing, and effects on the river ecosystem. *Hydrobiologia* 640:71–88. DOI: 10.1007/s10750-009-
651   0067-4.

652 Howard J, Sutton-Grier A, Herr D, Kleypas J, Landis E, Mcleod E, Pidgeon E, Simpson S. 2017.
653   Clarifying the role of coastal and marine systems in climate mitigation. *Frontiers in Ecology and the*
654   *Environment* 15:42–50. DOI: 10.1002/fee.1451.
655 IBGE – INSTITUTO BRASILEIRO DE GEOGRAFIA E ESTATÍSTICA. 2020. Censo Brasileiro de
656   2019. Rio de Janeiro: IBGE
657 Imchen M, Kumavath R. 2021. Metagenomic insights into the antibiotic resistome of mangrove
658   sediments and their association to socioeconomic status. *Environmental pollution* 268:115795. DOI:
659   10.1016/j.envpol.2020.115795.
660 Imchen M, Kumavath R, Barh D, Azevedo V, Ghosh P, Viana M, Wattam AR. 2017. Searching for
661   signatures across microbial communities: Metagenomic analysis of soil samples from mangrove and
662   other ecosystems. *Scientific reports* 7:8859. DOI: 10.1038/s41598-017-09254-6.
663 Imchen M, Kumavath R, Barh D, Vaz A, Góes-Neto A, Tiwari S, Ghosh P, Wattam AR, Azevedo V.
664   2018. Comparative mangrove metagenome reveals global prevalence of heavy metals and antibiotic
665   resistome across different ecosystems. *Scientific reports* 8:11187. DOI: 10.1038/s41598-018-29521-
666   4.
667 Kanehisa M, Sato Y. 2020. KEGG Mapper for inferring cellular functions from protein sequences.
668   *Protein science: a publication of the Protein Society* 29:28–35. DOI: 10.1002/pro.3711.
669 Karami A, Sarshar M, Ranjbar R, Zanjani RS. 2014. The Phylum Spirochaetaceae. In: Rosenberg E,
670   DeLong EF, Lory S, Stackebrandt E, Thompson F eds. *The Prokaryotes*. Berlin, Heidelberg: Springer
671   Berlin Heidelberg, 915–929. DOI: 10.1007/978-3-642-38954-2_156.
672 Kielak AM, Barreto CC, Kowalchuk GA, van Veen JA, Kuramae EE. 2016. The Ecology of
673   Acidobacteria: Moving beyond Genes and Genomes. *Frontiers in microbiology* 7:744. DOI:
674   10.3389/fmicb.2016.00744.
675 Kozich JJ, Westcott SL, Baxter NT, Highlander SK, Schloss PD. 2013. Development of a dual-index
676   sequencing strategy and curation pipeline for analyzing amplicon sequence data on the MiSeq
677   Illumina sequencing platform. *Applied and environmental microbiology* 79:5112–5120. DOI:
678   10.1128/AEM.01043-13.
679 Kristensen JM, Singleton C, Clegg L-A, Petriglieri F, Nielsen PH. 2021. High Diversity and Functional
680   Potential of Undescribed "Acidobacteriota" in Danish Wastewater Treatment Plants. *Frontiers in*
681   *microbiology* 12:643950. DOI: 10.3389/fmicb.2021.643950.
682 Lin X, Hetharua B, Lin L, Xu H, Zheng T, He Z, Tian Y. 2019. Mangrove Sediment Microbiome:
683   Adaptive Microbial Assemblages and Their Routed Biogeochemical Processes in Yunxiao Mangrove
684   National Nature Reserve, China. *Microbial ecology* 78:57–69. DOI: 10.1007/s00248-018-1261-6.
685 Liu P, Conrad R. 2017. Syntrophobacteraceae-affiliated species are major propionate-degrading sulfate
686   reducers in paddy soil. *Environmental microbiology* 19:1669–1686. DOI: 10.1111/1462-2920.13698.
687 Lopes NS. 2011. Análise da paisagem com base na fragmentação - caso APA do Pratigi, baixo sul da
688   Bahia, Brasil. *Revista Eletrônica do Prodema* 6:53–67.
689 Louca S, Doebeli M. 2018. Efficient comparative phylogenetics on large trees. *Bioinformatics* 34:1053–
690   1055. DOI: 10.1093/bioinformatics/btx701.
691 Macreadie PI, Anton A, Raven JA, Beaumont N, Connolly RM, Friess DA, Kelleway JJ, Kennedy H,
692   Kuwae T, Lavery PS, Lovelock CE, Smale DA, Apostolaki ET, Atwood TB, Baldock J, Bianchi TS,
693   Chmura GL, Eyre BD, Fourqurean JW, Hall-Spencer JM, Huxham M, Hendriks IE, Krause-Jensen D,
694   Laffoley D, Luisetti T, Marbà N, Masque P, McGlathery KJ, Megonigal JP, Murdiyarso D, Russell

695   BD, Santos R, Serrano O, Silliman BR, Watanabe K, Duarte CM. 2019. The future of Blue Carbon
696   science. *Nature communications* 10:3998. DOI: 10.1038/s41467-019-11693-w.
697   Marchandin H, Jumas-Bilak E. 2014. The Family Veillonellaceae. In: Rosenberg E, DeLong EF, Lory S,
698   Stackebrandt E, Thompson F eds. *The Prokaryotes: Firmicutes and Tenericutes*. Berlin, Heidelberg:
699   Springer Berlin Heidelberg, 433–453. DOI: 10.1007/978-3-642-30120-9_361.
700   Marcos MS, Barboza AD, Keijzer RM, Laanbroek HJ. 2018. Tide as Steering Factor in Structuring
701   Archaeal and Bacterial Ammonia-Oxidizing Communities in Mangrove Forest Soils Dominated by
702   Avicennia germinans and Rhizophora mangle. *Microbial ecology* 75:997–1008. DOI:
703   10.1007/s00248-017-1091-y.
704   Mascarenhas RB, Aragão IR, Reis P, de Jesus Bomfim T. 2019. ANÁLISE DE METAIS-TRAÇOS EM
705   SEDIMENTOS DA APA DO PRATIGI, BAHIA. *Sitientibus. Serie Ciencias Biologicas* 0. DOI:
706   10.13102/sitientibus.v0i53.4467.
707   McDonald D, Price MN, Goodrich J, Nawrocki EP, DeSantis TZ, Probst A, Andersen GL, Knight R,
708   Hugenholtz P. 2012. An improved Greengenes taxonomy with explicit ranks for ecological and
709   evolutionary analyses of bacteria and archaea. *The ISME journal* 6:610–618. DOI:
710   10.1038/ismej.2011.139.
711   MDMA, Ministério do Meio Ambiente. 2010. Plano Territorial de Desenvolvimento Sustentável do
712   Território Baixo Sul da Bahia. http://sit.mda.gov.br/download/ptdrs/ptdrs_qua_territorio021.pdf
713   Meyer DD, de Andrade PAM, Durrer A, Andreote FD, Corção G, Brandelli A. 2016. Bacterial
714   communities involved in sulfur transformations in wastewater treatment plants. *Applied microbiology*
715   *and biotechnology* 100:10125–10135. DOI: 10.1007/s00253-016-7839-3.
716   MMA, Ministério do Meio Ambiente. 2004. Plano de Manejo da APA do Pratigi - Encarte II Zoneamento
717   e Plano de Gestao.
718   Moitinho MA, Bononi L, Souza DT, Melo IS, Taketani RG. 2018. Bacterial Succession Decreases
719   Network Complexity During Plant Material Decomposition in Mangroves. *Microbial ecology*
720   76:954–963. DOI: 10.1007/s00248-018-1190-4.
721   Mori K, Suzuki K-I. 2014. The Family Thioalkalispiraceae. In: Rosenberg E, DeLong EF, Lory S,
722   Stackebrandt E, Thompson F eds. *The Prokaryotes: Gammaproteobacteria*. Berlin, Heidelberg:
723   Springer Berlin Heidelberg, 653–658. DOI: 10.1007/978-3-642-38922-1_399.
724   Morton JT, Sanders J, Quinn RA, McDonald D, Gonzalez A, Vázquez-Baeza Y, Navas-Molina JA, Song
725   SJ, Metcalf JL, Hyde ER, Lladser M, Dorrestein PC, Knight R. 2017. Balance Trees Reveal
726   Microbial Niche Differentiation. *mSystems* 2. DOI: 10.1128/mSystems.00162-16.
727   Nelson DW, Sommers LE. 1996. Total Carbon, Organic Carbon, and Organic Matter: Part 3 Chemical
728   Methods. In: Sparks DL, Page AL, Helmke PA, Loeppert RH, Soltanpour PN, Tabatabai MA,
729   Johnston CT, Sumner ME eds. *Methods of Soil Analysis*. SSSA Book Series. Madison, WI, USA: Soil
730   Science Society of America, American Society of Agronomy, 961–1010. DOI:
731   10.2136/sssabookser5.3.c34.
732   Nesme J, Achouak W, Agathos SN, Bailey M, Baldrian P, Brunel D, Frostegård Å, Heulin T, Jansson JK,
733   Jurkevitch E, Kruus KL, Kowalchuk GA, Lagares A, Lappin-Scott HM, Lemanceau P, Le Paslier D,
734   Mandic-Mulec I, Murrell JC, Myrold DD, Nalin R, Nannipieri P, Neufeld JD, O'Gara F, Parnell JJ,
735   Pühler A, Pylro V, Ramos JL, Roesch LFW, Schloter M, Schleper C, Sczyrba A, Sessitsch A, Sjöling
736   S, Sørensen J, Sørensen SJ, Tebbe CC, Topp E, Tsiamis G, van Elsas JD, van Keulen G, Widmer F,
737   Wagner M, Zhang T, Zhang X, Zhao L, Zhu Y-G, Vogel TM, Simonet P. 2016. Back to the Future of
738   Soil Metagenomics. *Frontiers in microbiology* 7:73. DOI: 10.3389/fmicb.2016.00073.

739 Nie S, Zhang Z, Mo S, Li J, He S, Kashif M, Liang Z, Shen P, Yan B, Jiang C. 2021. Desulfobacterales
740   stimulates nitrate reduction in the mangrove ecosystem of a subtropical gulf. *The Science of the total*
741   *environment* 769:144562. DOI: 10.1016/j.scitotenv.2020.144562.
742 Ottoni JR, Cabral L, de Sousa STP, Júnior GVL, Domingos DF, Soares Junior FL, da Silva MCP, Marcon
743   J, Dias ACF, de Melo IS, de Souza AP, Andreote FD, de Oliveira VM. 2017. Functional
744   metagenomics of oil-impacted mangrove sediments reveals high abundance of hydrolases of
745   biotechnological interest. *World journal of microbiology & biotechnology* 33:141. DOI:
746   10.1007/s11274-017-2307-5.
747 Parada AE, Needham DM, Fuhrman JA. 2016. Every base matters: assessing small subunit rRNA primers
748   for marine microbiomes with mock communities, time series and global field samples. *Environmental*
749   *microbiology* 18:1403–1414. DOI: 10.1111/1462-2920.13023.
750 Paulson JN, Stine OC, Bravo HC, Pop M. 2013. Differential abundance analysis for microbial marker-
751   gene surveys. *Nature methods* 10:1200–1202. DOI: 10.1038/nmeth.2658.
752 Pereira M. 2016. Espacialização geoquímica dos sedimentos do estuário do Rio Serinhaém, baixo sul da
753   Bahia – Brasil / geochemical spacialization of the sediments of the Rio Serinhaém estuary, lower
754   south of Bahia - Brazil. Programa de Pós-Graduação em Modelagem em Ciências da Terra e do
755   Ambiente – PPGM Thesis. Universidade Estadual de Feira de Santana.
756 R Core Team. 2019. R: A Language and Environment for Statistical Computing.
757 Ribeiro M, Aguiar WM, Nunes LA, Carneiro LDS. 2019. Morphometric Changes in Three Species of
758   Euglossini (Hymenoptera: Apidae) in Response to Landscape Structure. DOI:
759   10.13102/sociobiology.v66i2.3779.
760 Röling WFM. 2014. The Family Geobacteraceae. In: Rosenberg E, DeLong EF, Lory S, Stackebrandt E,
761   Thompson F eds. *The Prokaryotes: Deltaproteobacteria and Epsilonproteobacteria*. Berlin,
762   Heidelberg: Springer Berlin Heidelberg, 157–172. DOI: 10.1007/978-3-642-39044-9_381.
763 Sanders CJ, Eyre BD, Santos IR, Machado W, Luiz-Silva W, Smoak JM, Breithaupt JL, Ketterer ME,
764   Sanders L, Marotta H, Silva-Filho E. 2014. Elevated rates of organic carbon, nitrogen, and
765   phosphorus accumulation in a highly impacted mangrove wetland. *Geophysical Research Letters*
766   41:2475–2480. DOI: 10.1002/2014gl059789.
767 de Santana CO, Spealman P, Melo VMM, Gresham D, de Jesus TB, Chinalia FA. 2021. Effects of tidal
768   influence on the structure and function of prokaryotic communities in the sediments of a pristine
769   Brazilian mangrove. *Biogeosciences* 18:2259–2273. DOI: 10.5194/bg-18-2259-2021.
770 Santos IS, Nolasco M. 2017. Modelagem de Fundo do Estuário do Serinhaém – Ba: Morfologia e
771   Granulometria / Modeling of the bottom of Serinhaém's estuary, BA: Morphology and Granulometry.
772   Caderno de Geografia 27:247. DOI: 10.5752/p.2318-2962.2017v27n49p247.
773 Schriewer A, Miller WA, Byrne BA, Miller MA, Oates S, Conrad PA, Hardin D, Yang H-H, Chouicha N,
774   Melli A, Jessup D, Dominik C, Wuertz S. 2010. Presence of Bacteroidales as a predictor of pathogens
775   in surface waters of the central California coast. *Applied and environmental microbiology* 76:5802–
776   5814. DOI: 10.1128/AEM.00635-10.
777 Seeley ME, Song B, Passie R, Hale RC. 2020. Microplastics affect sedimentary microbial communities
778   and nitrogen cycling. *Nature communications* 11:2372. DOI: 10.1038/s41467-020-16235-3.
779 Spalding M, Kainuma M, Collins L. 2010. World Atlas of Mangroves (version 3.1). A collaborative
780   project of ITTO, ISME, FAO, UNEP-WCMC, UNESCO-MAB, UNU-INWEH and TNC. London
781   (UK): Earthscan, London. URL: http://www.routledge.com/books/details/9781844076574, Data DOI:
782   https://doi.org/10.34892/w2ew-m83

783   Sun S, Jones RB, Fodor AA. 2020. Inference-based accuracy of metagenome prediction tools varies
784   across sample types and functional categories. Microbiome 8:46. DOI: 10.1186/s40168-020-00815-y.
785   Trevathan-Tackett SM, Sherman CDH, Huggett MJ, Campbell AH, Laverock B, Hurtado-McCormick V,
786   Seymour JR, Firl A, Messer LF, Ainsworth TD, Negandhi KL, Daffonchio D, Egan S, Engelen AH,
787   Fusi M, Thomas T, Vann L, Hernandez-Agreda A, Gan HM, Marzinelli EM, Steinberg PD, Hardtke
788   L, Macreadie PI. 2019. A horizon scan of priorities for coastal marine microbiome research. Nature
789   ecology & evolution 3:1509–1520. DOI: 10.1038/s41559-019-0999-7.
790   Ullah R, Yasir M, Khan I, Bibi F, Sohrab SS, Al-Ansari A, Al-Abbasi F, Al-Sofyani AA, Daur I, Lee S-
791   W, Azhar EI. 2017. Comparative bacterial community analysis in relatively pristine and
792   anthropogenically influenced mangrove ecosystems on the Red Sea. *Canadian journal of*
793   *microbiology* 63:649–660. DOI: 10.1139/cjm-2016-0587.
794   Vavourakis CD, Mehrshad M, Balkema C, van Hall R, Andrei A-Ş, Ghai R, Sorokin DY, Muyzer G.
795   2019. Metagenomes and metatranscriptomes shed new light on the microbial-mediated sulfur cycle in
796   a Siberian soda lake. *BMC biology* 17:69. DOI: 10.1186/s12915-019-0688-7.
797   Wang L, Huang X, Zheng T-L. 2016. Responses of bacterial and archaeal communities to nitrate
798   stimulation after oil pollution in mangrove sediment revealed by Illumina sequencing. Marine
799   pollution bulletin 109:281–289. DOI: 10.1016/j.marpolbul.2016.05.068.
800   Wang C, Hu R, Strong PJ, Zhuang W, Huang W, Luo Z, Yan Q, He Z, Shu L. 2021. Prevalence of
801   antibiotic resistance genes and bacterial pathogens along the soil–mangrove root continuum. Journal
802   of hazardous materials 408:124985. DOI: 10.1016/j.jhazmat.2020.124985.
803   Weiss S, Xu ZZ, Peddada S, Amir A, Bittinger K, Gonzalez A, Lozupone C, Zaneveld JR, Vázquez-
804   Baeza Y, Birmingham A, Hyde ER, Knight R. 2017. Normalization and microbial differential
805   abundance strategies depend upon data characteristics. *Microbiome* 5:27. DOI: 10.1186/s40168-017-
806   0237-y.
807   Whitman WB, Bowen TL, Boone DR. 2014. The Methanogenic Bacteria. In: Rosenberg E, DeLong EF,
808   Lory S, Stackebrandt E, Thompson F eds. *The Prokaryotes: Other Major Lineages of Bacteria and*
809   *The Archaea*. Berlin, Heidelberg: Springer Berlin Heidelberg, 123–163. DOI: 10.1007/978-3-642-
810   38954-2_407.
811   Ye Y, Doak TG. 2009. A parsimony approach to biological pathway reconstruction/inference for
812   genomes and metagenomes. *PLoS computational biology* 5:e1000465. DOI:
813   10.1371/journal.pcbi.1000465.
814   Yun J, Deng Y, Zhang H. 2017. Anthropogenic protection alters the microbiome in intertidal mangrove
815   wetlands in Hainan Island. *Applied microbiology and biotechnology* 101:6241–6252. DOI:
816   10.1007/s00253-017-8342-1.
817   Zhou Z, Meng H, Liu Y, Gu J-D, Li M. 2017. Stratified Bacterial and Archaeal Community in Mangrove
818   and Intertidal Wetland Mudflats Revealed by High Throughput 16S rRNA Gene Sequencing.
819   *Frontiers in microbiology* 8:2148. DOI: 10.3389/fmicb.2017.02148.
820

Figure 1

Location map of the collection sites of the pristine and impacted mangrove areas.

Figure 2

Taxonomic abundances of prokaryotes in each mangrove site.

Summed normalized read abundances from across replicates of prokaryotic groups for phylum and class taxonomic levels at each mangrove site.
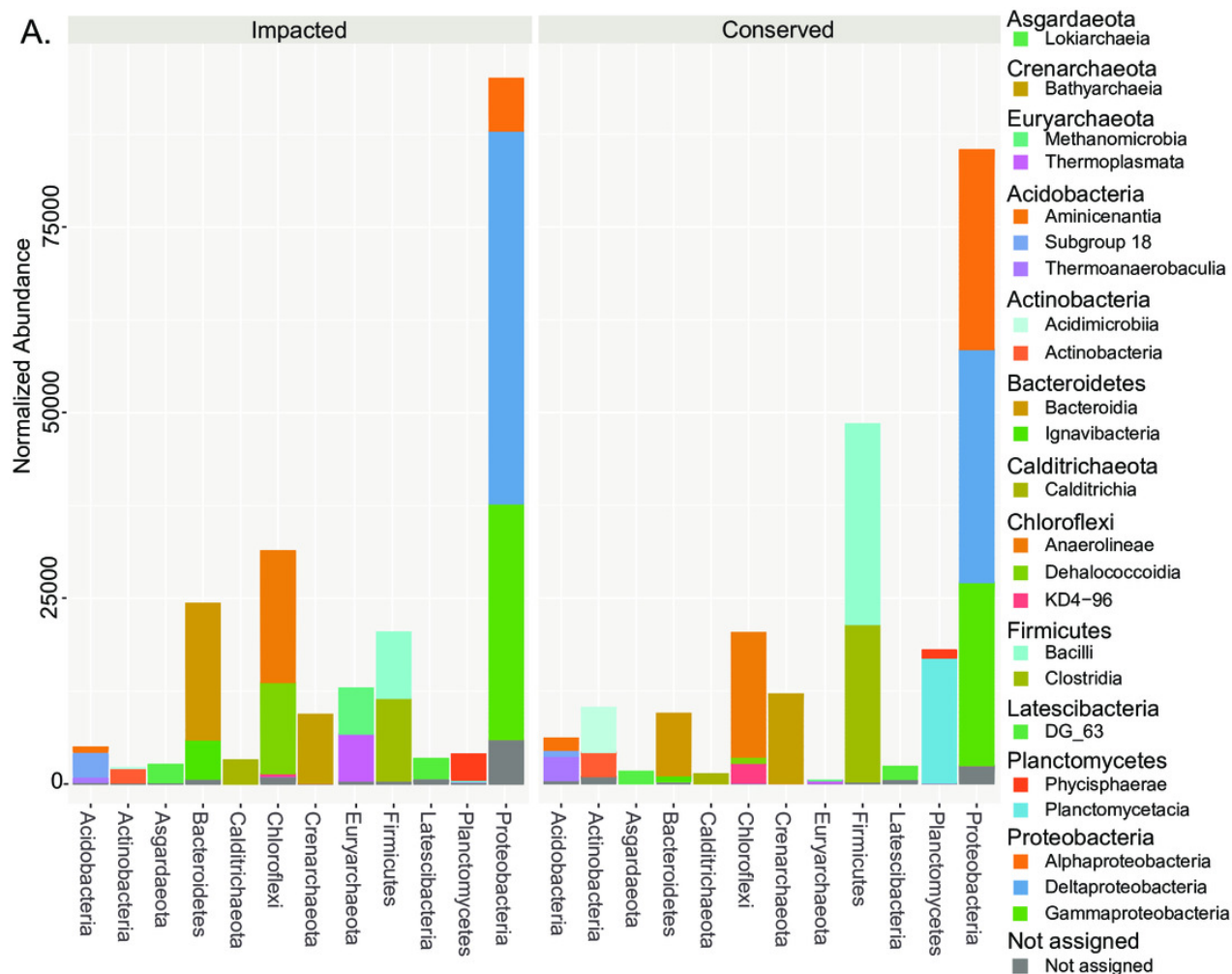
Figure 3

Prokaryotic diversity and environmental factors interacting to create distinct communities.

Here we show Total ASVs per site (A), alpha-diversity using Shannon's Index (B), and beta-diversity using Bray-Curtis (C). A PCoA plot of the sample sites with fitted vectors of environmental variables (D) shows Organic matter, Temperature, and Cu are significantly correlated with the prokaryotic communities, while Dissolved oxygen, pH, Ba, and Salinity are marginally significant.

Figure D content:

Variable	p-value
Organic Matter	0.04
Temperature	0.05
Cu	0.05
Dissolved Oxygen	0.07
pH	0.07
Ba	0.10
Salinity+	0.10
Fe	0.11
Zn	0.16
V	0.38
Co	0.40
Pb	0.45
As	0.50
Sn	0.50
Cr	0.52
Mn	0.53
Ni	0.58
Al	0.77
Li	0.87
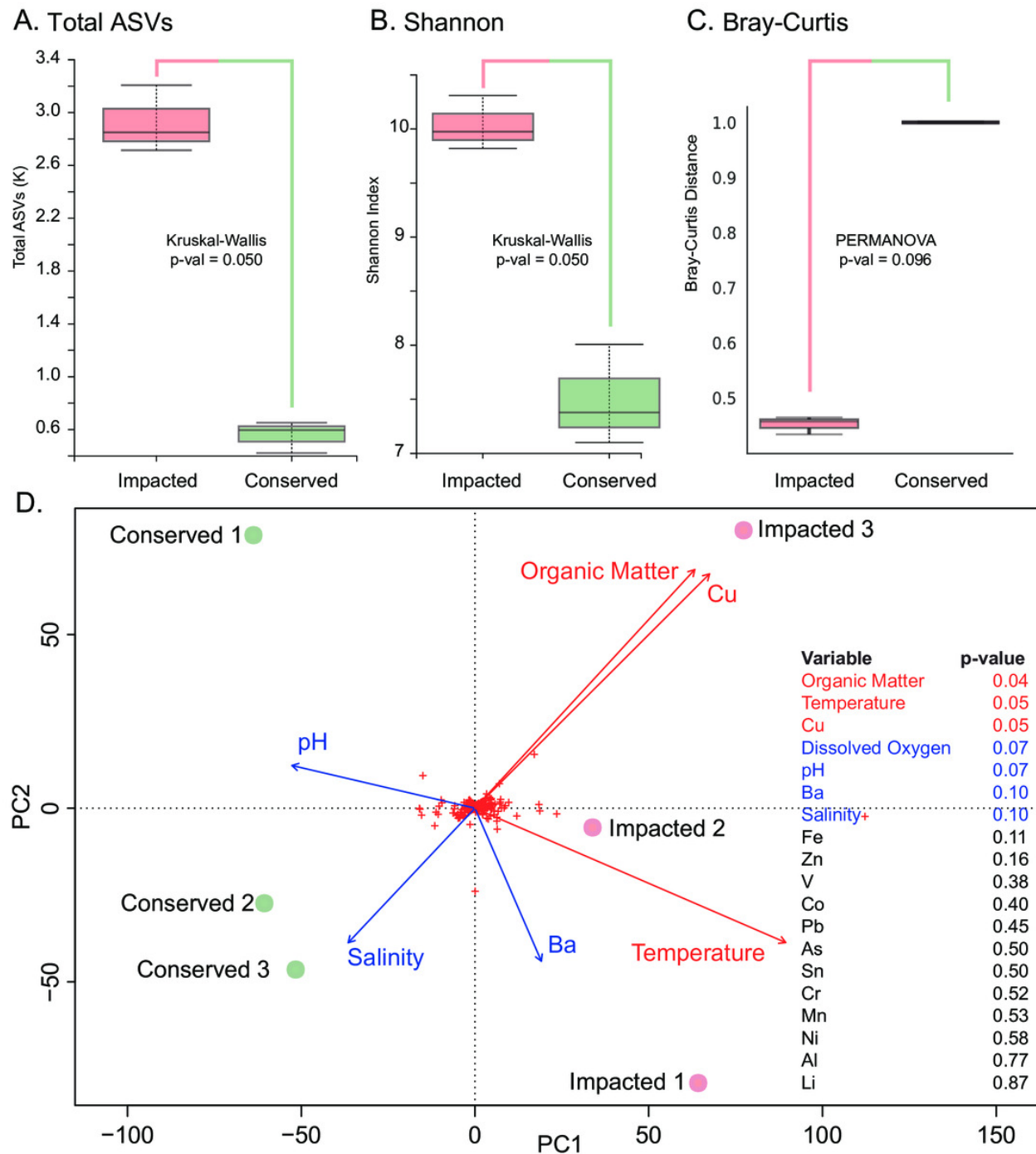
Figure 4

Taxa with significant differences between impacted and conserved mangrove sites

Prokaryotic families with significant differences in abundances and large effect size differences (>20%) between the mangrove sites. Some families show zero abundance in one of the studied areas.

Median Log10 Normalized Taxa Abundance
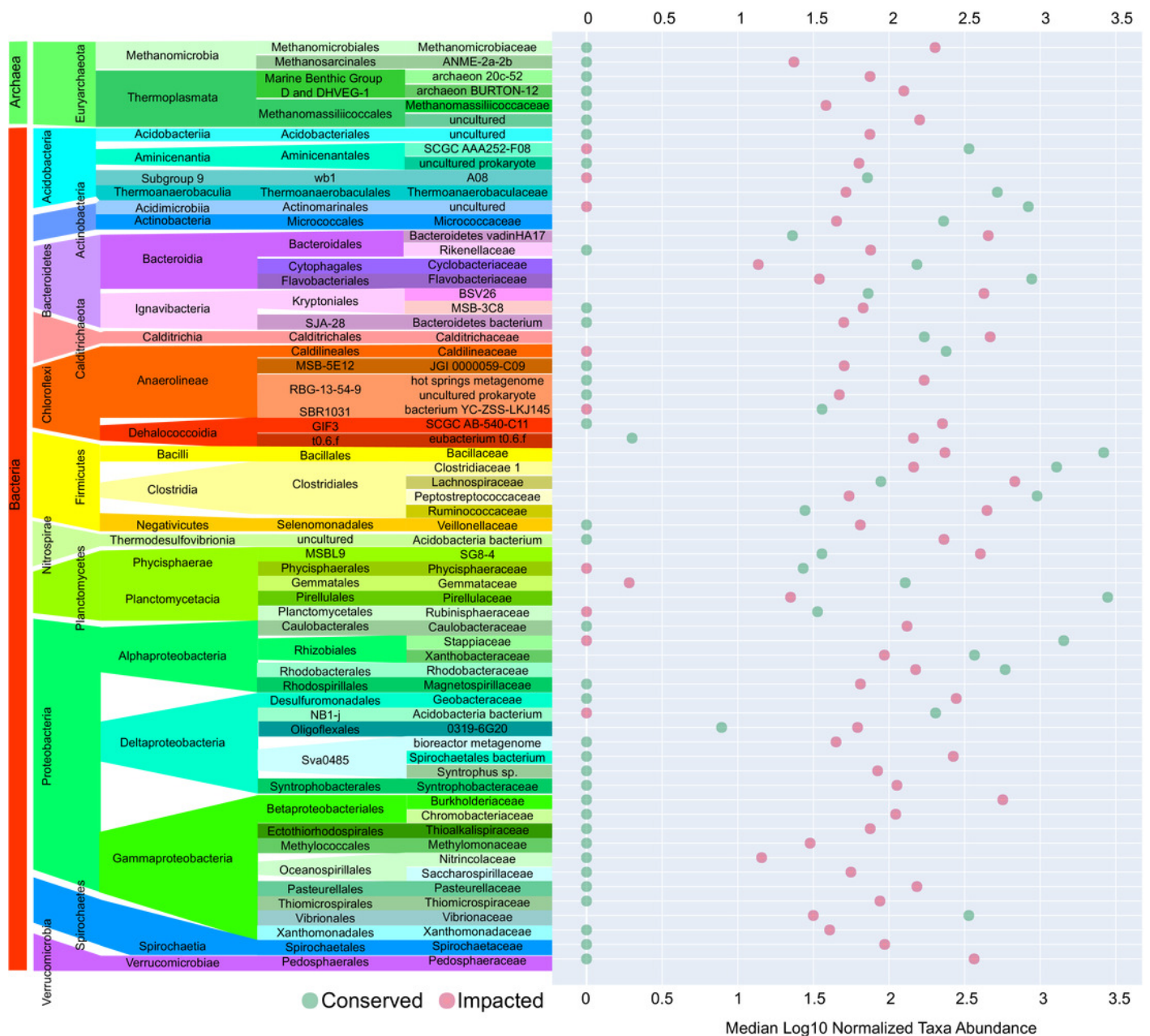
Figure 5

Carbon metabolism pathways and different abundances between sites.

Abundance heatmaps of carbon metabolic pathways in each site. (A) carbon fixation for photosynthetic organisms. (B) carbon fixation for not photosynthetic organisms. (C) methane metabolism. (D) photosynthesis.

A.
Methane metabolism

Methane metabolism (cont.)

B.
Carbon fixation in prokaryotes

C. Carbon fixation in photosynthetic organisms

Conserved   Impacted

Conserved   Impacted
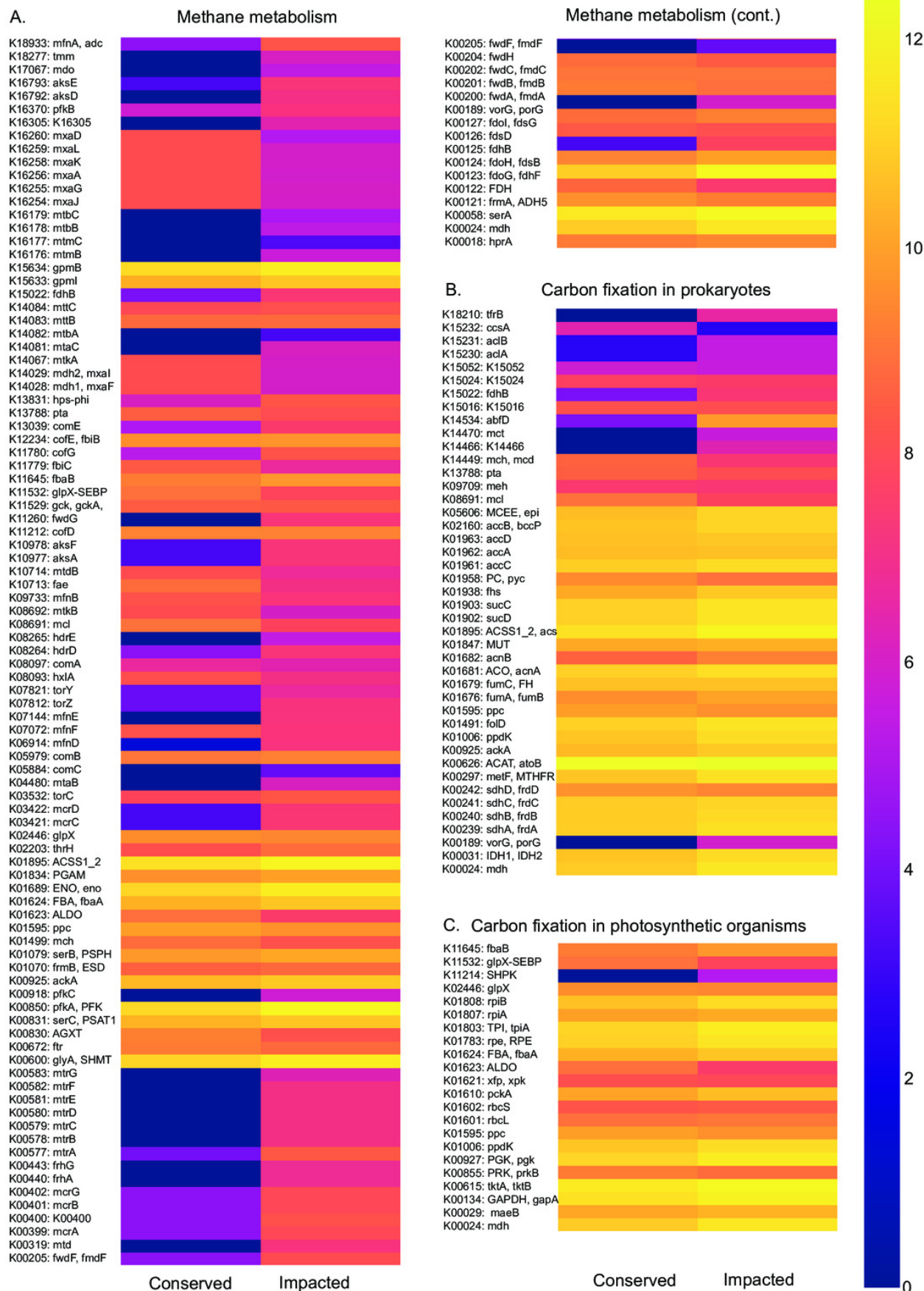
Figure 6

Abundances of metabolic pathways of different elements at each site.

Heatmaps of metabolic pathways abundances for nitrogen (A), sulfur (B), pentose phosphate (C), photosynthesis (D).
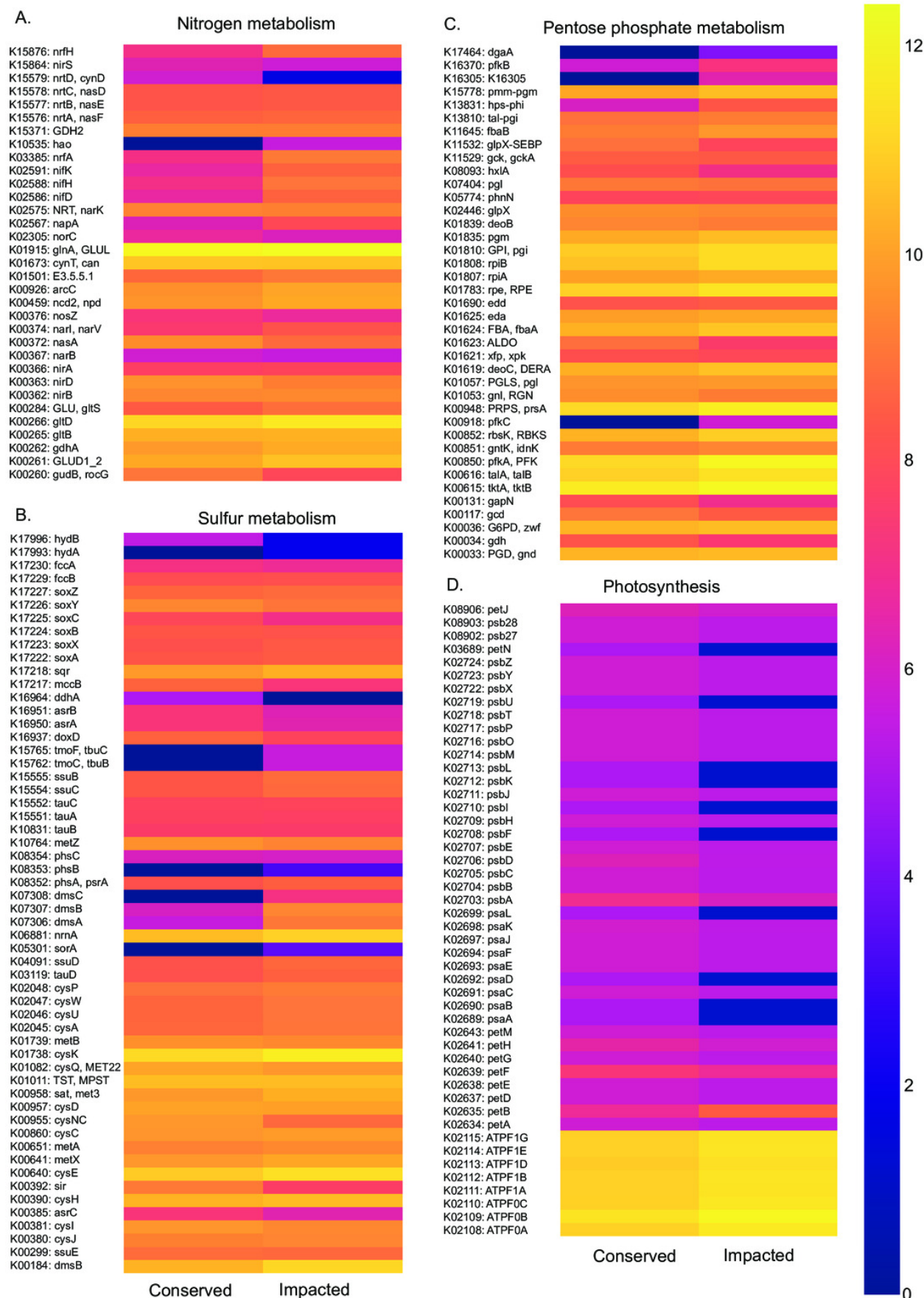
Figure 7

Taxa responsible for the metabolic potentials.

Relative contributions of the prokaryotic families that contribute for > 5% of the metabolic potentials in at least one site.

Carbon Fixation in Prokaryotes
Carbon Fixation in Photosynthetic Organisms
Methane
Nitrogen Metabolism
Pentose Phosphate Metabolism
Photosynthesis
Sulfur

Impacted
Conserved

Bacillaceae

Syntrophaceae*

Anaerolineaceae*

Desulfarculaceae

Stappiaceae

Desulfobacteraceae

0   2   4   6   8   10   12   14   16

Percent Relative Abundance
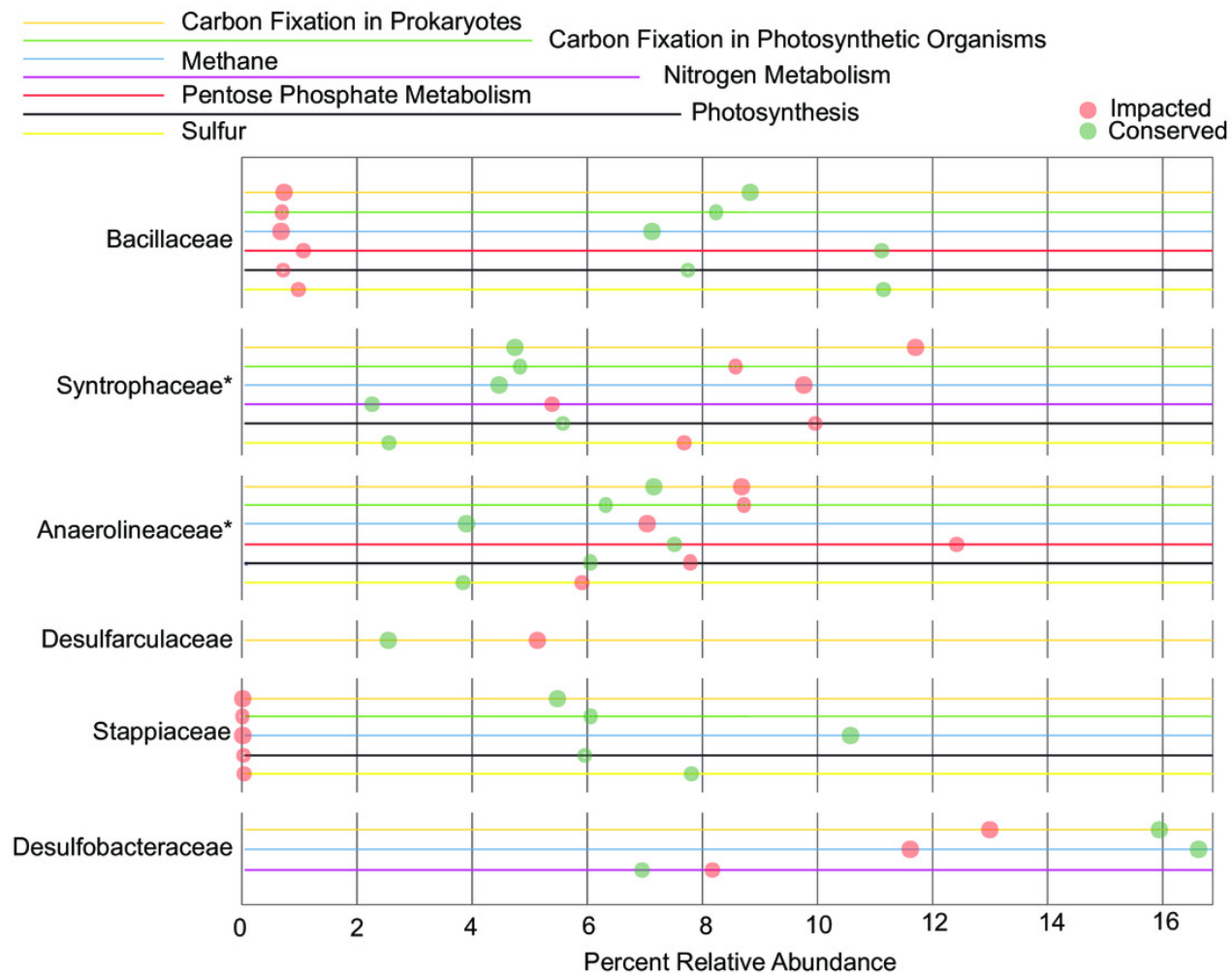
*These families had median NSTI values within 1 standard deviation of 0.15